ELSEVIER

Journal of Crystal Growth 234 (2002) 359–363

JOURNAL OF CRYSTAL GROWTH

www.elsevier.com/locate/jcrysgro

(Ga,Mn,As) compounds grown on semi-insulating GaAs with mass-analyzed low energy dual ion beam deposition

Junling Yang[a,*], NuoFu Chen[a,b], Zhikai Liu[a], Shaoyan Yang[a], Chunlin Chai[a], Meiyong Liao[a], Hongjia He[a]

[a] *Laboratory of Semiconductor Materials Science, Institute of Semiconductor, Chinese Academy of Sciences, P.O. Box 912, Beijing 100083, People's Republic of China*

[b] *National Microgravity Laboratory of the Chinese Academy of Sciences, People's Republic of China*

Received 20 August 2001; accepted 5 September 2001
Communicated by M. Schieber

Abstract

The (Ga,Mn,As) compounds were obtained by the implantation of Mn ions into semi-insulating GaAs substrate with mass-analyzed low energy dual ion beam deposition technique. Auger electron spectroscopy depth profile of a typical sample grown at the substrate temperature of 250°C showed that the Mn ions were successfully implanted into GaAs substrate with the implantation depth of 160 nm. X-ray diffraction was employed for the structural analyses of all samples. The experimental results were greatly affected by the substrate temperature. $Ga_{5.2}Mn$ was obtained in the sample grown at the substrate temperature of 250°C. $Ga_{5.2}Mn$, Ga_5Mn_8 and Mn_3Ga were obtained in the sample grown at the substrate temperature of 400°C. However, there is no new phase in the sample grown at the substrate temperature of 200°C. The sample grown at 400°C was annealed at 840°C. In this annealed sample Mn_3Ga disappeared, Ga_5Mn_8 tended to disappear, $Ga_{5.2}Mn$ crystallized better and a new phase of Mn_2As was generated.

PACS: 81.05.Ea; 81.05.Zx; 81.15.Hi; 61.66.Dk; 61.82.Fk

Keywords: A1. X-ray diffraction; A3. Ion beam epitaxy; B2. Gallium arsenide

1. Introduction

In the field of modern information technology, semiconductor and magnetic materials are both very important. Semiconductor devices take advantage of the charge of electron to process information, whereas magnetic devices such as magnetic tape take advantage of the spin of electron to record information. If the charge and spin of the electron can be combined, then it is possible to further enhance the performance of magnetic devices and semiconductor devices and prepare new types of functional devices. Furthermore, the storage and processing of information

*Corresponding author. Tel.: +86-10-82304627; fax: +86-10-82304469.

E-mail address: yjl@red.semi.ac.cn (J. Yang).

0022-0248/02/$ - see front matter
PII: S0022-0248(01)01722-5

may be carried out at the same time. So it is very significant to integrate magnetic and semiconducting properties [1].

Up to now, there are two approaches to integrate magnetic and semiconducting properties. One is to prepare diluted magnetic semiconductor, in which a large amount of magnetic ions are incorporated into a compound semiconductor [2–4]. The other approach is to prepare magnet/semiconductor hybrid structures. There are two kinds of magnet/semiconductor hybrid structures. One is obtained by preparing epitaxial magnetic thin film on semiconductor substrates [5–13], the other involves embedding magnetic particles in a semiconductor substrate to form a kind of granular film [14,15].

As an important semiconductor material, GaAs is extensively used in high speed electronic devices and optoelectronic devices. If we can prepare GaAs-based diluted magnetic semiconductors or magnet/GaAs hybid structure, then magnetic phenomena can be introduced into conventional nonmagnetic GaAs-based optical and electrical devices.

In this paper, (Ga,Mn,As) compounds—Ga–Mn and Mn–As phases—were grown on semi-insulating GaAs substrates by the implantation of magnetic elemental Mn into GaAs substrate at certain substrate temperatures with mass-analyzed low energy dual ion beam deposition technique.

2. Material preparation

Samples were prepared by mass-analyzed low energy dual ion beam deposition apparatus which consists of ion beam systems and vacuum systems. One of its advantages is to purify ions by its magnetic analyzer.

Mn ions were uniformly deposited on semi-insulating GaAs (0 0 1) with Mn ion energy of 1000 eV and a dose of 1.5×10^{18} Mn^+/cm^2. All GaAs substrates were etched and cleaned before sample growth. Purity of Mn used in the experiment was 99.98%. Mn did not need to be etched and cleaned because of the purifying function of the growing apparatus itself. In order to remove the absorbed impurities on the surface of the GaAs substrate, the substrate was bombarded by Argon ion for 10 min. During the growth, the GaAs substrates were heated to the scheduled temperature (200°C for sample 1, 250°C for sample 2 and 400°C for sample 3). It took 60 min to grow each sample.

Sample 3 was annealed at an atmosphere of flowing N_2 at 840°C in an automatically temperature-conditioned annealing furnace for 70 min and the flowing rate of N_2 is 0.5 l/min. During the annealing process, the sample surface clings to a polished GaAs wafer so as to prevent Mn from evaporating from the sample surface.

3. Measurement and analyses

In order to investigate the structure and distribution of Mn ions along the depth, X-ray diffraction (XRD) and Auger electron spectroscopy (AES) were employed for structural and compositional analyses.

3.1. Compositional analyses

AES was employed for analyzing the surface composition of sample 2 and its compositional variation along the cross section. The AES system used in this experiment is PHI-610/SAM. In order to analyze elemental composition at the sample surface, it was measured with AES. The AES spectra showed that there is manganese, gallium, arsenic, carbon, sulfur and oxygen at the sample surface (see Fig. 1).

Fig. 2 is the AES depth profile of sample 2, from which it can be seen that the concentration of element Mn reaches the maximum at a depth of 30 nm. The reason for the existance of carbon and sulfur is that the sample surface was contaminated after the sample was taken from the growth chamber. The element oxygen was introduced by oxidation of manganese after the sample was taken from the growth chamber. At the sample surface, the concentration of oxygen is as high as 48% indicating that Mn is easily oxidized. Although the oxygen is very high at the surface, it decreases rapidly along the depth. During the whole analyzed depth area, the relative concentration of

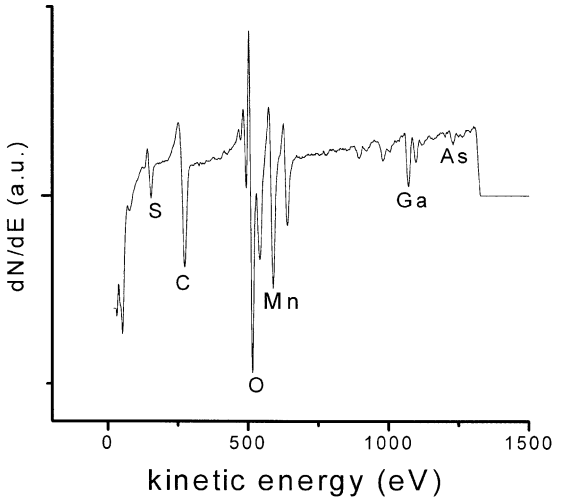

Fig. 1. Auger electron spectroscopy spectra at the surface of sample 2.

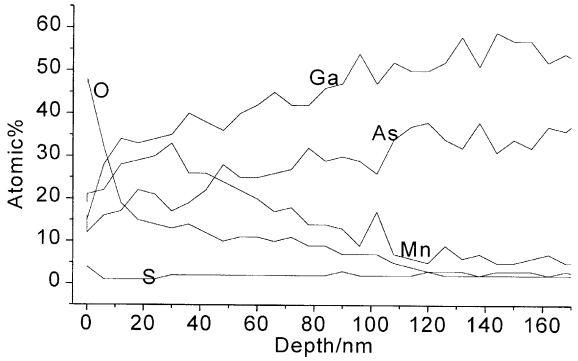

Fig. 2. Auger electron spectroscopy depth profile of sample 2.

Mn does not monotonically decrease, indicating that there is a segregation of Mn atoms in the sample.

3.2. Structural analyses

XRD patterns of the sample were measured with $2\theta-\theta$ scan using Cu K_α radiation for structural analyses. Fig. 3 is the XRD spectra of sample 1, from which it can be seen that there is no new phase in sample 1. Fig. 4 is the XRD spectra of sample 2, from which it can be seen that there are two new phases, $Ga_{5.2}Mn$ and γ-Mn_2O_3. The structure system of $Ga_{5.2}Mn$ is orthorhombic with the lattice constants $a = 5.299$ nm, $b = 5.381$ nm

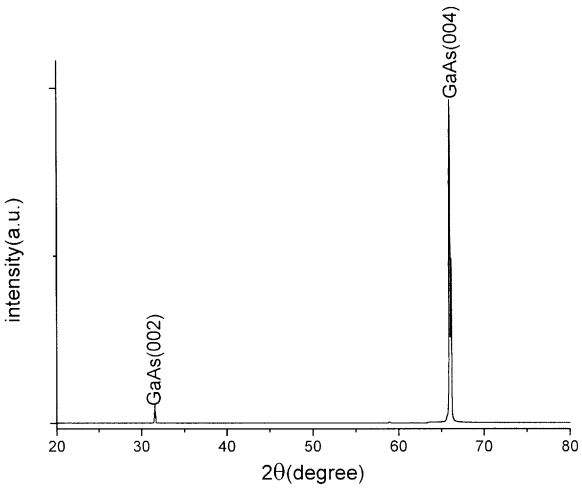

Fig. 3. X-ray diffraction spectra of sample 1.

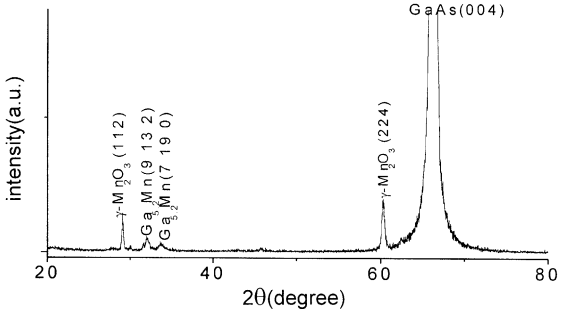

Fig. 4. X-ray diffraction spectra of sample 2.

and $c = 0.994$ nm. In Fig. 4, the highest peak is from the diffraction of GaAs (0 0 4). At the left of GaAs (0 0 4) peak, there are four peaks which are in sequence from the diffraction of γ-Mn_2O_3 (1 1 2), $Ga_{5.2}Mn$ (9 13 2), $Ga_{5.2}Mn$ (7 19 0) and γ-Mn_2O_3 (2 2 4). Fig. 5 is the XRD spectra of sample 3, from which it can be seen that there are four phases except GaAs, $Ga_{5.2}Mn$, Ga_5Mn_8, α-Mn and Mn_3Ga. The crystal structure of α-Mn is FCC with lattice constant $a = 0.89121$ nm. The structure of Ga_5Mn_8 is the cubic system with the lattice constant $a = 0.8992$ nm. The structure of Mn_3Ga is hexagonal with the lattice constants $a = 0.5404$ nm and $c = 0.4357$ nm. In Fig. 5, the highest peak is from the diffraction of GaAs (0 0 4). At the left of GaAs (0 0 4) peak, there are seven diffraction peaks which are in sequence from

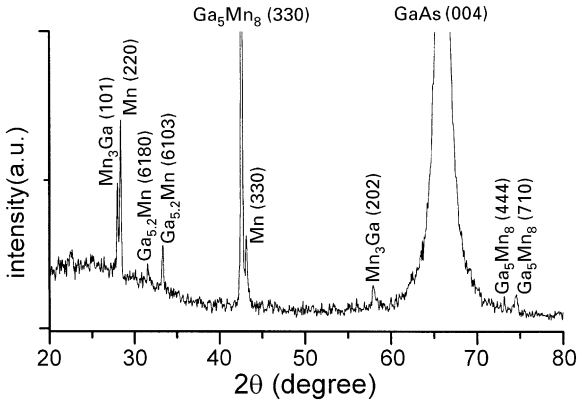

Fig. 5. X-ray diffraction spectra of sample 3 before annealing.

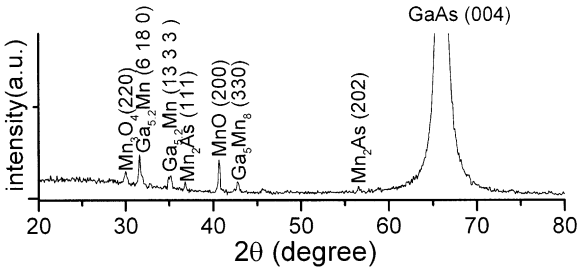

Fig. 6. X-ray diffraction spectra of sample 3 after annealing.

the diffraction of Mn_3Ga (1 0 1), α-Mn (2 2 0), $Ga_{5.2}Mn$ (6 18 0), $Ga_{5.2}Mn$ (6 10 3), Ga_5Mn_8 (3 3 0), α-Mn (3 3 0) and Mn_3Ga (2 0 2). At the right of GaAs (0 0 4) peak, there are diffraction peaks of Ga_5Mn_8 (4 4 4) and Ga_5Mn_8 (7 1 0). The peak of Ga_5Mn_8 (3 3 0) in sample 3 is very strong and narrow indicating that the growth conditions of sample 3 are quite suited to the nucleation and growth of Ga_5Mn_8.

These XRD patterns showed that there are new Ga–Mn compounds in both samples 2 and 3 and there is no new phase in sample 1. Furthermore, there are more compounds of Ga_5Mn_8, α-Mn and Mn_3Ga in sample 3 than in sample 2. It is evident that the substrate temperature is critical to the formation and disappearance of Ga–Mn and Mn–As compounds. The reason for the appearance of α-Mn peak in sample 3 is that the implanted Mn is crystallized better because of the high substrate temperature compared with samples 1 and 2.

Fig. 6 is the XRD spectra of sample 3 after annealing, from which it can be seen that there are five phases besides GaAs, $Ga_{5.2}Mn$, Ga_5Mn_8, Mn_2As, Mn_3O_4 and MnO. The crystal system of Mn_2As is tetragonal with the lattice constants $a = 0.3767$ nm and $c = 0.6277$ nm. In Fig. 5, the highest peak is from the diffraction of GaAs (0 0 4). At the left of GaAs (0 0 4) peak, there are eight diffraction peaks which are in sequence from the diffraction of Mn_3O_4 (2 2 0), $Ga_{5.2}Mn$ (6 18 0), $Ga_{5.2}Mn$ (13 3 3), Mn_2As (1 1 1), MnO (2 0 0), Ga_5Mn_8 (3 3 0) and Mn_2As (2 0 2). After annealing at 840°C, Mn_3O_4, MnO and Mn_2As appeared, whereas Mn_3Ga and α-Mn disappeared. Mn_3O_4 and MnO are the products of oxidation of Mn due to the intake of oxygen into the annealing atmosphere. Furthermore, manganese oxides may crystallize well at a high annealing temperature. The appearance of Mn_2As shows that Mn_2As can nucleate and grow at the high temperature of 840°C. The disappearance of α-Mn resulted partially from the combination of Mn with the elements Ga and As, and partially resulted from the oxidation of Mn at the high temperature of 840°C. The disappearance of Mn_3Ga suggests that Mn_3Ga is not stable at 840°C. At the same time, the intensity peak of Ga_5Mn_8 largely decreases, indicating that Ga_5Mn_8 is also unstable at 840°C. After annealing, the diffraction peaks of $Ga_{5.2}Mn$ become slightly stronger and sharper, indicating that $Ga_{5.2}Mn$ is crystallized better during annealing. The annealing was beneficial to the growth of $Ga_{5.2}Mn$ and Mn_2As.

According to the above results, $Ga_{5.2}Mn$ is the only new compound in the sample grown at a low temperature of 250°C. At the same time, $Ga_{5.2}Mn$ existed in the sample grown at 400°C and crystallized better during annealing at 840°C. These facts indicate that it is easy for $Ga_{5.2}Mn$ to nucleate and grow and $Ga_{5.2}Mn$ is stable over a wide range of temperatures.

4. Summary

(Ga,Mn,As) compounds were obtained with mass-analyzed low energy dual ion beam

deposition with Mn ion energy of 1000 eV and a dose of 1.5×10^{18} Mn^+/cm^2. The substrate temperature is very important in preparing samples. There is a difference between the samples grown at different substrate temperatures. There was no new phase in the sample grown at 200°C. There is only one Ga–Mn phase, $Ga_{5.2}Mn$, in the sample grown at 250°C and there are three Ga–Mn phases, $Ga_{5.2}Mn$, Ga_5Mn_8 and Mn_3Ga, in the sample grown at 400°C. After the sample grown at 400°C was annealed at 840°C, the Mn_3Ga disappeared, Ga_5Mn_8 tends to disappear, Mn_2As appeared and $Ga_{5.2}Mn$ crystallized better. The annealing was beneficial to the growth of $Ga_{5.2}Mn$ and Mn_2As. It is also evident that $Ga_{5.2}Mn$ is stable over a wide range of temperatures.

Acknowledgements

This work was partially supported by special funds for Major State Basic Research Project G20000683, and by the Ministry of Chinese National Science and Technology under contract PAN95-YU-34.

References

[1] H. Ohno, Science 281 (1998) 951.
[2] H. Ohno, Appl. Phys. Lett. 69 (1996) 363.
[3] W. Van Roy, H. Akinaga, S. Miyanishi, K. Tanaka, L.H. Kuo, J. Magn. Magn. Mater. 165 (1997) 149.
[4] T. Hayashi, M. Tanaka, K. Seto, T. Nishinaga, K. Ando, Appl. Phys. Lett. 71 (1997) 1825.
[5] J.R. Waldrop, R.W. Grant, Appl. Phys. Lett. 34 (1979) 630.
[6] G.A. Prinz, J.J. Krebs, Appl. Phys. Lett. 39 (1981) 397.
[7] G.A. Prinz, Science 250 (1990) 1092.
[8] G.A. Prinz, Phys. Today (Special Issue on Magnetoelectronics) 48 (1995) 58.
[9] M. Tanaka, J. Crystal Growth 201/202 (1999) 660.
[10] P.M. Thibaro, E. Kneedler, B.T. Jonker, B.R. Bennett, B.V. Shanabrook, L.J. Whitman, Phys. Rev. B 53 (1996) R10481.
[11] T. Sands, J.P. Harbison, M.L. Leadbeater, S.J. Allen, G.W. Hull, R. Ramesh, V.G. Keramidas, Appl. Phys. Lett. 57 (1990) 2609.
[12] M. Tanaka, J.P. Harbison, M.C. Park, Y.S. Park, T. Shin, M. Rothberg, Appl. Phys. Lett. 65 (1994) 1964.
[13] S. Miyanishi, H. Akinaga, W. VanRoy, K. Tanaka, Appl. Phys. Lett. 70 (1997) 2046.
[14] E.E. Fullerton, J.E. Mattson, S.R. Lee, C.H. Sowers, Y.Y. Huang, G. Felcher, S.D. Bader, F.T. Parker, J. Magn. Magn. Mater. 117 (1992) L301.
[15] H. Akinaga, J. De Boeck, G. Borghs, Appl. Phys. Lett. 72 (25) (1998) 3368.